Plasticized solid polymer electrolyte based on triblock copolymer poly(vinylidene chloride-*co*-acrylonitrile-*co*-methyl methacrylate) for magnesium ion batteries

T. Ponraj, et al. *[full author details at the end of the article]*

Abstract

Limited global resources of lithium lead to the consideration of magnesium ion batteries as potential energy storage devices. Magnesium ion batteries have potential for high energy density but require new types of electrode and electrolytes for practical applications. Solid polymer electrolytes offer the opportunity for increased safety and broader electrochemical stability relative to traditional electrolytes. Herein, we report the development of solid polymer electrolyte for magnesium ion batteries based on triblock copolymer poly(vinylidene chloride-*co*-acrylonitrile-*co*-methyl methacrylate) (poly(VdCl-*co*-AN-*co*-MMA)). The polymer electrolytes are prepared by solution-casting technique using poly(VdCl-*co*-AN-*co*-MMA) with various concentrations (10 wt%, 20 wt%, 30 wt%, and 40 wt%) of magnesium chloride ($MgCl_2$) salt. Among the prepared polymer electrolytes, the highest magnesium-ion-conducting polymer electrolyte is 70 wt% poly(VdCl-*co*-AN-*co*-MMA):30 wt% $MgCl_2$ polymer–salt composition by electrochemical impedance measurements, and the obtained value of ionic conductivity is found to be in the order of 10^{-5} S cm^{-1}. Addition of plasticizer succinonitrile in various concentrations (0.1 wt%, 0.2 wt%, 0.3 wt% and 0.4 wt%) with the identified polymer electrolyte of highest conductivity shows increased values of conductivity up to the order of 10^{-3} S cm^{-1}. Observable changes in crystalline/amorphous nature of the polymer are analyzed using X-ray diffraction pattern. Glass transition temperature of polymer electrolytes has been found using differential scanning calorimetric studies. Transference number measurements have been made to confirm the ionic conductivity. The electrochemical stability for highest conducting plasticized polymer electrolyte is obtained from linear sweep voltammetry as 3.3 V. A primary magnesium ion battery has been constructed with prepared electrolyte of highest conductivity, and its performance and discharge characteristics are also analyzed. The open-circuit voltage of 2.18 V is obtained with the constructed primary magnesium ion battery.

Keywords Polymer electrolyte · Magnesium battery · Triblock copolymer · Electrochemical device · Magnesium chloride · Succinonitrile

Introduction

At present, extensive energy storage devices are required to efficiently store the electrical energy produced from different sources. Rechargeable batteries need improvements for better performance in various applications. The rechargeable battery network requires a material that is low cost, safe, and more capable to store energy. However, the lithium-ion battery satisfies the primary requirements, but the demand for rechargeable batteries increases continuously because of the limitations of lithium like cost and availability. The search for new materials for battery application includes magnesium which has numerous advantages over lithium. Abundance of magnesium in earth crust is 10^4 times more when compared to lithium. Magnesium has greater theoretical volumetric capacity of 3833 mAh/cm^3 due its two-electron reduction. Additional advantage of magnesium includes low cost, more stability in air, safe operation with wide range of temperatures, and non-dendritic electrochemical performance [1–8]. No distinct volume changes occurred during charge–discharge cycling in magnesium ion batteries because the magnesium ion has same ionic radius as that of lithium [9]. Due to these benefits, magnesium ion batteries acquire more attention, and an advanced investigation is necessary so as to develop the batteries to fulfill the energy storage requirements. The major concern in the progress of magnesium ion batteries is finding appropriate electrolytes which are compatible with magnesium electrodes [10]. Basically, conventional liquid electrolytes offer better ionic conductivity, but they face a lot of drawbacks in safety concerns. Most of the liquid electrolytes are flammable and has high toxicity [11]. Solid polymer electrolytes (SPEs) have been paid an attention as promising materials for electrochemical devices [12, 13]. Polymer host materials as the solid matrix with the addition of alkali or alkaline metal salt without any trace of liquid organic solvents constitute SPEs [14]. The advantages of SPEs include no leakage, very low flammability, high flexibility, high safety, high compliance, and stable contact between the electrodes and electrolyte [15–17]. SPEs have very strong adhesive property with the surface of electrodes compared to the conventional liquid electrolytes, and thus they have less interface impedance between electrolyte and electrodes. The basic requirements for SPEs used in battery applications comprise high mechanical strength, greater thermal stability, high ionic conductivity at room temperature, and wide-ranging electrochemical stability [18, 19].

Among various types of SPEs, block copolymers (BCPs) provides a way to achieve both high ionic conductivity and mechanical stability. The BCP consists of different blocks which are chemically dissimilar polymers and connected endwise by covalent bond. The microphase separation occurring between the dissimilar polymers in BCP splits the blocks into periodically nano-spaced domains. One block may contain ionic moieties which are tethered together with polymer backbone and other blocks provide mechanical support [20, 21]. In the case of BCP electrolytes, many recent researches have been found for diblock and triblock copolymers with lithium salts for lithium-ion batteries [22–28]. Didier Devaux et al. studied comb and linear triblock copolymers with

lithium salt using polystyrene and poly(ethylene oxide) polymers. In this study, it is concluded that comb block copolymer electrolytes (BCEs) have slightly better ionic conductivity than linear BCEs at room temperature. But, electrochemical stability window at 80 °C of these BCEs is poor, and the linear BCEs show good performance during battery tests [22]. DigantaSaikia and coworkers reported the ionic conductivity of plasticized blend polymer electrolytes based on poly(vinylidene fluoride-*co*-hexafluoropropylene) and triblock copolymer poly(propylene glycol)–block–poly(ethylene glycol)–block–poly(propylene glycol) bis(2-aminopropyl ether) diamine for lithium-ion batteries as in the order of 10^{-2} S cm^{-1} [23]. Nicholas P. Young et al. analyzed the performance of polypropylene–block–poly(ethylene oxide)–block–syndiotactic polypropylene triblock copolymers with lithium bis(trifluoromethane) sulfonimide salt and proven their unusual performance as solid polymer electrolytes [24]. Wen-Shiue Young and Thomas H. Epps demonstrated the benefits of block copolymer systems with 3-D conducting pathways for electrolyte membranes by investigating the conductivity studies of poly(styrene-*b*-ethylene oxide) (PS–PEO) samples with lithium perchlorate (LiClO$_4$) [25]. Charge transport in nanostructured triblock copolymer electrolytes based on poly(ethylene oxide) and polystyrene has been analyzed with theoretical predictions by R. Bouchet et al. [26]. Sebnem Inceoglu and coworkers reported the ionic conductivity at low temperatures below 50 °C as in the order of 10^{-7} S cm^{-1} and 10^{-4} S cm^{-1} at higher temperatures up to 90 °C for poly(ethylene oxide)-*b*-polystyrenesulfonyllithium(trifluoromethylsulfonyl)imide (PEO–PSLiTFSI) diblock copolymers [27]. The triblock copolymer material based on poly(styrene trifluoromethanesulphonylimide of lithium) P(STFSILi) and poly(ethylene oxide) (PEO) is studied as a polymer electrolyte which exhibits exceptional levels of performance for lithium–metal batteries in terms of ionic conductivity in the order of 10^{-4} S cm^{-1} [28].

Poly(vinylidene chloride-*co*-acrylonitrile-*co*-methyl methacrylate) (poly(VdCl-*co*-AN-*co*-MMA)), the triblock copolymer electrolytes containing ammonium and lithium salts, has been studied by very few research groups. The great advantages of the triblock copolymer poly(VdCl-*co*-AN-*co*-MMA) include the hydrophobic nature and occurrence of huge number of polar groups such as oxygen, nitrogen, and chlorine in the copolymer which is responsible for the enhanced ionic mobility [29–32]. Addition of plasticizers has been used to enhance the conductivity of many copolymers with various salts [33]. For the first time, the present work deals with the aim of developing the plasticized triblock copolymer electrolyte for magnesium ion batteries using poly(VdCl-*co*-AN-*co*-MMA) polymer, magnesium chloride (MgCl$_2$) salt, and succinonitrile (SN) plasticizer. Initially, the polymer electrolytes are prepared using the triblock copolymer and magnesium salt. The polymer electrolyte of the highest conductivity among prepared electrolytes has been selected for the further enhancement of ionic conductivity using the plasticizer, and the plasticized polymer electrolytes are characterized with various characterization techniques.

Materials and methods

Preparation of polymer electrolytes

The polymer electrolyte samples using triblock copolymer poly(VdCl-*co*-AN-*co*-MMA) have been prepared by solution-casting method with tetrahydrofuran (THF) as solvent. Poly(VdCl-*co*-AN-*co*-MMA) (molecular weight (MW): 250.1), magnesium chloride (MW: 203.31), succinonitrile (MW: 80.09), and tetrahydrofuran are purchased from Sigma-Aldrich. Prior to the preparation of polymer electrolyte samples, both poly(VdCl-*co*-AN-*co*-MMA) powder and magnesium chloride ($MgCl_2$) salt are dried in the vacuum chamber at 100 °C for 12 h. Appropriate amount of poly(VdCl-*co*-AN-*co*-MMA) is dissolved in THF under constant stirring at room temperature. Required amount of $MgCl_2$ is dissolved separately with 1 ml of water to obtain an aqueous solution of $MgCl_2$ and added with poly(VdCl-*co*-AN-*co*-MMA)/THF solution. A homogeneous viscous liquid is obtained after continues stirring for 12 h. The homogeneous viscous liquids with various concentrations of poly(VdCl-*co*-AN-*co*-MMA) and $MgCl_2$ are poured into identical glass petri dishes and allowed to dry in room temperature for 24 h. The solvent-free polymer electrolyte films with a thickness of 1 mm to 2 mm are obtained, and the films are further dried in a vacuum chamber at 60 °C to remove any traces of solvent or water content. The prepared polymer electrolytes are pure poly(VdCl-*co*-AN-*co*-MMA), 90 wt% poly(VdCl-*co*-AN-*co*-MMA):10 wt% $MgCl_2$, 80 wt% poly(VdCl-*co*-AN-*co*-MMA):20 wt% $MgCl_2$, 70 wt% poly(VdCl-*co*-AN-*co*-MMA):30 wt% $MgCl_2$, and 60 wt% poly(VdCl-*co*-AN-*co*-MMA):40 wt% $MgCl_2$.

(Hereafter poly(VdCl-*co*-AN-*co*-MMA) is abbreviated as P(VdCl…))

In addition to these prepared polymer electrolytes, the plasticized polymer electrolytes are prepared using the plasticizer succinonitrile (SN). SN with different concentrations (0.1 wt%, 0.2 wt%, 0.3 wt%, 0.4 wt%) is added separately with homogeneous mixture of 70 wt% P(VdCl…) and 30 wt% $MgCl_2$ under constant stirring at room temperature. The solvent-free plasticized polymer electrolytes obtained with polymer–salt–plasticizer compositions are 70 wt% P(VdCl…):30 wt% $MgCl_2$:0.1 wt% SN, 70 wt% P(VdCl…):30 wt% $MgCl_2$:0.2 wt% SN, 70 wt% P(VdCl…):30 wt% $MgCl_2$:0.3 wt% SN, 70 wt% P(VdCl…):30 wt% $MgCl_2$:0.4 wt% SN. Figure 1 shows the photograph of 70 wt% P(VdCl…):30 wt% $MgCl_2$:0.3 wt% SN polymer membrane.

Fig. 1 Photograph of highest
conducting polymer membrane,
70 wt% P(VdCl…): 30 wt%
MgCl$_2$: 0.3 wt% SN
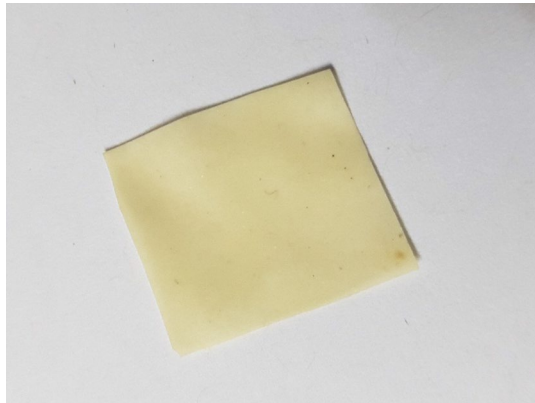
Characterization techniques

Structural analysis

X-ray diffraction (XRD) measurements have been carried out using Philips X'Pert PRO diffractometer by Cu-Kα radiations at room temperature with diffraction angle 2θ ranging from 10° to 90° at a rate of 2° min^{-1} to determine the extent of crystalline/amorphous nature of the polymer electrolyte samples.

Thermal analysis

Thermograms of prepared polymer electrolyte samples with heating rate of 10 °C/min have been obtained by differential scanning calorimetry (DSC) using DSC Q20 V24.10 Build 122 instrument to analyze the variation of glass transition temperature with concentration of salt/plasticizer in the polymer electrolyte samples.

Impedance spectroscopy analysis

Using HIOKI 3532–50 LCR HITESTER, the alternating current (AC) impedance measurements have been carried out in the frequency range of 42 Hz to 1 MHz with the electrolyte samples sandwiched between two stainless-steel blocking electrodes having the contact area of 4.0 cm^2.

Transference number measurements

Transference number measurements have been made using Wagner's DC polarization technique and Evan's polarization method to find out the charged species involved in the electrical conduction through the polymer electrolyte.

Linear sweep voltammetry

The linear sweep voltammetry responses of the highest conducting sample have been carried out using biologic science instruments VSP-300, France, by placing the sample between two stainless-steel electrodes at the scan rate of 1×10^{-3} Vs^{-1} in the potential range of 0–5 V.

Construction of primary magnesium battery

The primary battery has been constructed with prepared magnesium-ion-conducting polymer electrolyte sample of the highest conductivity using suitable electrodes. The anode–electrolyte–cathode assembly is firmed in a sample holder, and the output measurements have been taken from end to end. Magnesium metal with the thickness of 1 mm is used as anode.

Manganese oxide (MnO_2) with graphite is used as cathode material. MnO_2 powder and graphite powder are mixed together in the ratio of 3:1 and ground well. The homogeneous mixture of MnO_2 and graphite is pressed with 5-ton pressure using pelletizer to obtain pellet which is used as a cathode.

Fig. 2 XRD pattern of (a) pure P(VdCl…), (b) 70 wt% P(VdCl…): 30 wt% $MgCl_2$, (c) 70 wt% P(VdCl…): 30 wt% $MgCl_2$: 0.1 wt% SN, (d) 70 wt% P(VdCl…): 30 wt% $MgCl_2$: 0.2 wt% SN, (e) 70 wt% P(VdCl…): 30 wt% $MgCl_2$: 0.3 wt% SN, (f) 70 wt% P(VdCl…): 30 wt% $MgCl_2$: 0.4 wt% SN
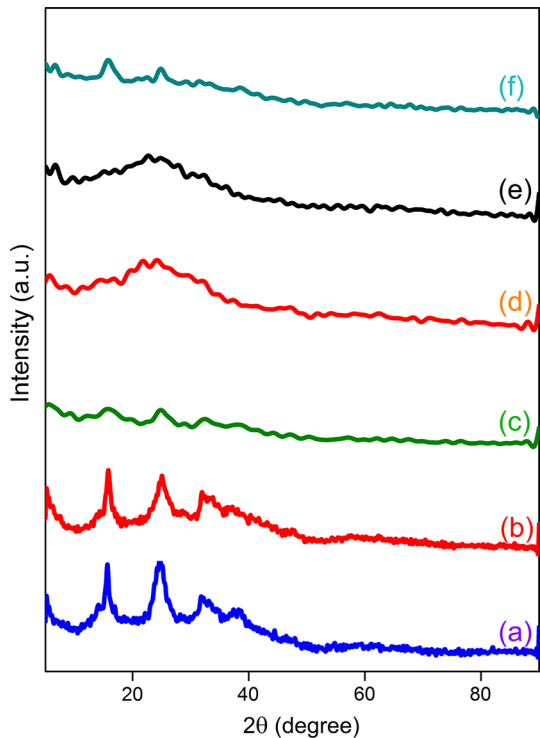
Results and discussion

XRD analysis

Figure 2, curves a and b, denotes XRD pattern of pure P(VdCl…) and 70 wt% P(VdCl…):30 wt% $MgCl_2$, respectively. The curves c–f represents the XRD pattern of 70 wt% P(VdCl…):30 wt% $MgCl_2$:0.1 wt% SN, 70 wt% P(VdCl…):30 wt% $MgCl_2$:0.2 wt% SN, 70 wt% P(VdCl…):30 wt% $MgCl_2$:0.3 wt% SN, 70 wt% P(VdCl…):30 wt% $MgCl_2$:0.4 wt% SN, respectively. The observable intense peaks at $2\theta = 15.8°$, 24.8° and broad peaks at $2\theta = 33.5°$, 37.3° for pure P(VdCl…) reveal that the polymer has the semicrystalline nature. These values of 2θ observed for pure host polymer are compatible with the earlier report [29–32]. No characteristic peaks can be found for $MgCl_2$ in all the prepared samples, and this indicates the complete dissolution of $MgCl_2$ into the polymer matrix [34, 35]. With the addition of $MgCl_2$ to the polymer, the peaks at $2\theta = 15.8°$, 24.8° become less intense which indicates the enhancement of amorphous nature of the triblock copolymer. Addition of 0.1 wt% of plasticizer SN again reduces the intensity of the peaks and increases the broadness of the peaks. The peaks observed at $2\theta = 15.8°$, 24.8°, 33.5° for 70 wt% P(VdCl…):30 wt% $MgCl_2$:0.1 wt% get disappears, and only a broad peak appears for 0.2 wt% and 0.3 wt% of SN with polymer–salt composition. The existence of broad peak alone in the pattern illustrates the complete amorphous nature of the polymer electrolyte samples. However, further increase in plasticizer concentration to 0.4 wt%, the pattern shows the same low-intensity peaks at $2\theta = 15.8°$, 24.8°, 33.5° indicates the increase in crystalline nature. Hodge et al. related the intensity of peaks with the crystalline or amorphous nature of the material [36] as when the intensity of peak reduces and broadness increases, the amorphous nature increases. High amorphous nature provides the easy diffusion of ions through the polymer matrix and increases the mobility of ions [37].

DSC analysis

Differential scanning calorimetric thermograms for pure P(VdCl…), 70 wt% P(VdCl…):30 wt% $MgCl_2$ polymer–salt complex, and plasticized polymer electrolytes are shown in Fig. 3. The values of glass transition temperature (T_g) for prepared plasticized polymer electrolytes are provided in Table 1. The glass transition temperature (T_g) for 70 wt% P(VdCl…):30 wt% $MgCl_2$ is observed as 143.1 °C and is slightly lower than pure P(VdCl…) having the T_g value of 144.4 °C. On the addition of plasticizer with the highest conducting polymer electrolyte having the polymer–salt composition 70 wt% P(VdCl…):30 wt% $MgCl_2$, the T_g value decreases as the concentration of plasticizer increases from 0.1 wt% to 0.3 wt%. The lowest T_g value is observed for 70 wt% P(VdCl…):30 wt% $MgCl_2$:0.3 wt% SN polymer–salt–plasticizer composition. When concentration of plasticizer is increased to 0.4 wt%, the T_g value increases. The changes observed in the values of T_g of prepared plasticized polymer electrolytes specify the interaction between the polymer,
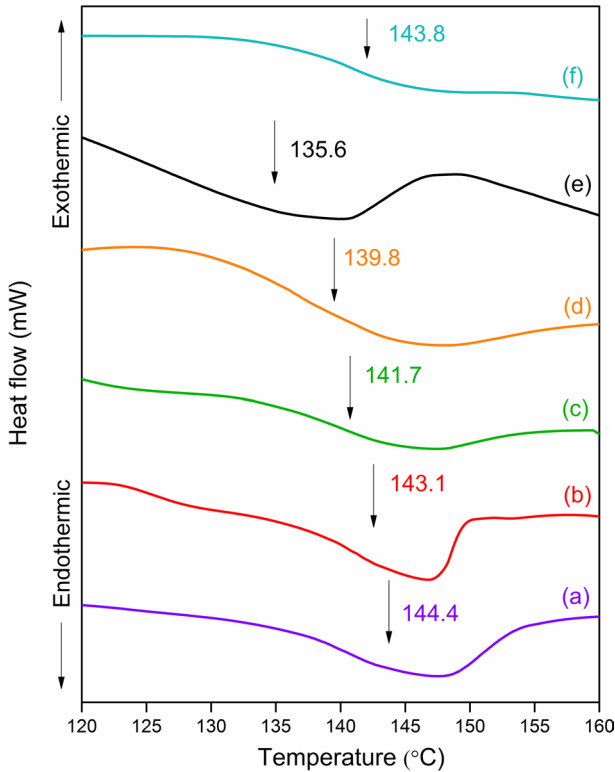
Fig. 3 DSC curves of (a) pure P(VdCl…), (b) 70 wt% P(VdCl…):30 wt% MgCl$_2$, (c) 70 wt% P(VdCl…): 30 wt% MgCl$_2$: 0.1 wt% SN, (d) 70 wt% P(VdCl…): 30 wt% MgCl$_2$: 0.2 wt% SN, (e) 70 wt% P(VdCl…): 30 wt% MgCl$_2$: 0.3 wt% SN, (f) 70 wt% P(VdCl…): 30 wt% MgCl$_2$: 0.4 wt% SN

Table 1 Glass transition temperature of polymer electrolytes

Compositions	T_g (°C)
Pure P(VdCl…)	144.4
70 wt% P(VdCl…):30 wt% MgCl$_2$	143.1
70 wt% P(VdCl…):30 wt% MgCl$_2$:0.1 wt% SN	141.7
70 wt% P(VdCl…):30 wt% MgCl$_2$:0.2 wt% SN	139.8
70 wt% P(VdCl…):30 wt% MgCl$_2$:0.3 wt% SN	135.6
70 wt% P(VdCl…):30 wt% MgCl$_2$:0.4 wt% SN	143.8

salt, and plasticizer. The plasticization effect takes place in the polymer electrolytes due to the addition of salt with polymer and thereby decreases the T_g values. The interactions between the dipoles among the chains in the polymer matrix get weakened with the addition of magnesium salt [38]. The polymer films get softened, and the segmental motion of the polymer chain increases due to the addition of salt [39, 40].

Electrochemical impedance analysis

AC impedance spectroscopy is a significant tool to study the electrical properties of the electrolyte or electrode materials. The ionic conductivity of the electrolyte is determined using AC impedance spectroscopy. The variation of AC impedance (Z) of the electrolyte with frequency (ω) at room temperature can be measured. A plot between the real and imaginary part of impedance as a function of frequency provides complex impedance plot or Nyquist plot or cole–cole plot. In general, the Nyquist plot consists of two distinct regions. Firstly, the semicircle at high-frequency region represents the bulk effect of the polymer electrolyte which is represented by an equivalent circuit with parallel combination of bulk capacitance and bulk resistance (R). Secondly, the inclined spike at low-frequency region is due to the effect of blocking double-layer capacitance at electrolyte–electrode interface by constant phase element (CPE) [41]. Figure 4a–c shows the Nyquist plot of prepared polymer electrolytes without plasticizer. It can be noted that for pure host polymer electrolyte, almost a complete semicircle is found. The semicircle gets diminished, while the concentration of magnesium salt has been increased, and the clear spike is observed at the end of semicircle. The EQ software developed by B.A. Boukamp [42, 43] is used to identify the exact value of bulk resistance in the Nyquist plot. The ionic conductivity (σ) of the prepared electrolytes can be calculated by

$$\sigma\left(\text{S cm}^{-1}\right) = \frac{t}{AR_\text{b}},$$

where t is the average thickness of a polymer electrolyte. "A" is the contact area between the polymer and the electrodes. R_b is the bulk resistance of the polymer electrolyte [44].

The ionic conductivity of polymer electrolytes without plasticizer at room temperature that has been determined by the values of bulk resistance obtained from Nyquist plots is provided in Table 2. The ionic conductivity at room temperature of pure P(VdCl…) is calculated as 3.07×10^{-8} S cm^{-1}. The conductivity values increases with increase in the concentration of magnesium salt. The highest conductivity of 1.89×10^{-5} S cm^{-1} is obtained for the polymer–salt composition, 70 wt% P(VdCl…):30 wt% MgCl$_2$. With further increase in salt concentration from 30 to 40 wt%, the conductivity value decreases. The decrease in conductivity is due to the formation of ion clusters and ion pairs [45].

Among all these prepared polymer electrolytes, the electrolyte of the highest conductivity has been chosen for the further enhancement of ionic conductivity by adding the plasticizer SN in various concentrations from 0.1 to 0.4 wt%. Figure 5 shows the Nyqusit plot of prepared plasticized polymer electrolytes. Only the spike region is observed for the highest conducting plasticized polymer electrolytes. The ionic conductivity obtained from Nyquist plot of plasticized polymer electrolytes is provided in Table 3. Ionic conductivity of the plasticized electrolyte samples has increased by two orders of magnitude than that of the electrolyte sample without plasticizer. The maximum value of ionic conductivity obtained is 1.42×10^{-3} S cm^{-1} for 70 wt% P(VdCl…):30 wt% MgCl$_2$:0.3 wt% SN polymer–salt–plasticizer

composition. When the plasticizer concentration is increased to 0.4 wt%, the conductivity decreases. The decrease in conductivity is due to the formation of ion clusters and ion pairs [45].

Conductance spectra analysis

The variation of logarithmic conductivity (log σ) with logarithmic angular frequency (log ω) gives the conduction spectra. The conduction spectra plot has three regions: low-frequency dispersion region, plateau region which is independent of frequency, and high-frequency dispersion region. The space-charge polarization that occurs at the blocking electrodes is responsible for the nature of curve at low-frequency region, and the curve at high-frequency region is due to the bulk relaxation phenomenon. The intersection of plateau region with log σ axis provides the information about DC conductivity of the electrolytes [46]. Figure 6 shows the conduction spectra of prepared plasticized polymer electrolytes. From the figure, only the low-frequency dispersion region and plateau region are observed in the conduction spectra of prepared plasticized polymer electrolytes. By extrapolating the plateau region of the curve on log σ axis, DC conductivity values of entire polymer electrolytes are obtained. The conductivity values obtained from the plot of conductance spectra agree with the results obtained from the Nyquist plot. The conductivity values obtained from Nyquist plot and conductance spectra are provided in Table 4.

Temperature-dependent conductivity studies

The variation of AC impedance of plasticized polymer electrolytes has been measured as a function of temperature ranges from 30 to 100 °C. Figure 7 shows the plot between logarithmic values of ionic conductivity (log σ) and reciprocal of corresponding temperatures (1000/T). The linear variation of ionic conductivity with temperature is observed which shows the Arrhenius behavior. The ionic conductivity of electrolyte samples is found to be increased with temperature. The expansion of polymer occurred during the rise in temperature which produces free volume to facilitate enhanced ionic mobility and segmental motion of polymer. [47]. The Arrhenius-type thermally activated process is governed by the relation:

$$\sigma = A \exp\left(\frac{-E_a}{kT}\right),$$

where A represents the constant of proportionality related to the amount of charge carriers, E_a represents the activation energy, k represents Boltzmann constant, and T represents the temperature. The regression values obtained from the linear fitting of the plot that are close to unity show the precision of linear fit, and the activation energy of all the electrolyte samples has been determined. Low activation energy is
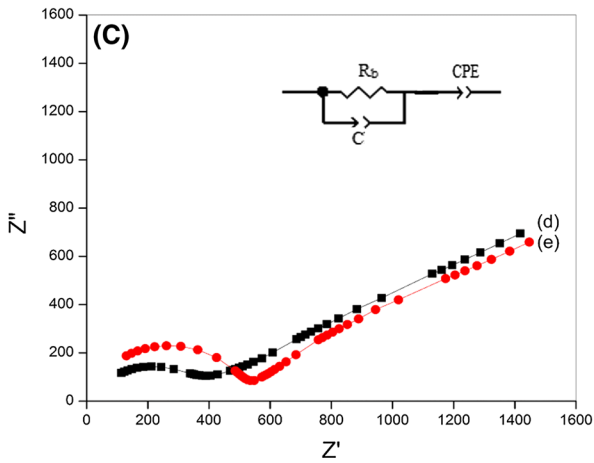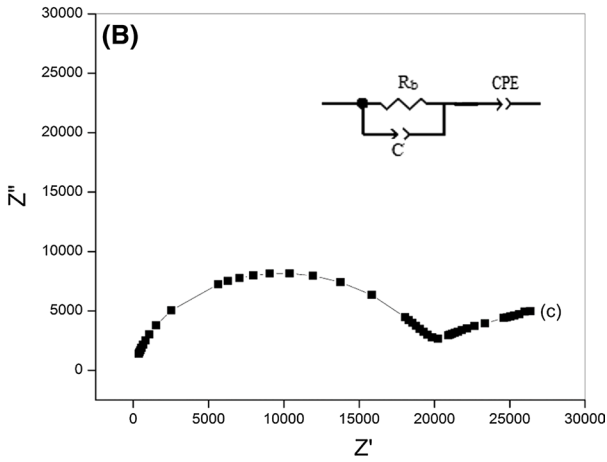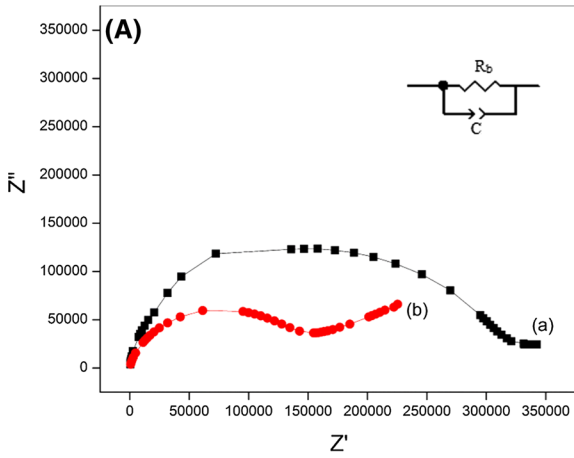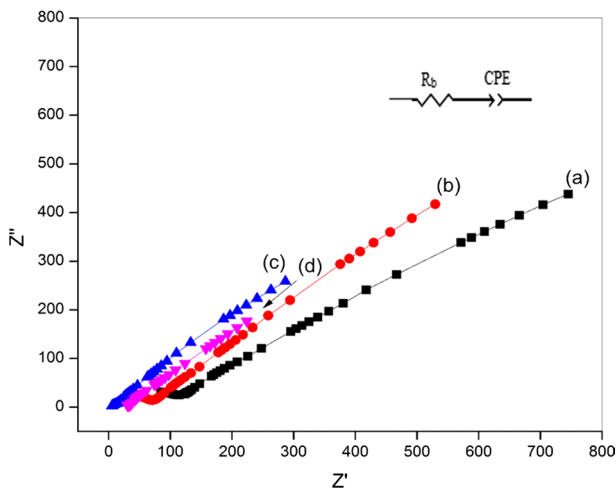
Table 2 Conductivity values calculated from Nyquist plot	Compositions	Ionic conductivity (σ) at room temperature S cm^{-1}
	Pure P(VdCl...)	3.07×10^{-8}
	90 wt% P(VdCl...):10 wt% MgCl$_2$	1.34×10^{-7}
	80 wt% P(VdCl...):20 wt% MgCl$_2$	5.50×10^{-7}
	70 wt% P(VdCl...):30 wt% MgCl$_2$	1.89×10^{-5}
	60 wt% P(VdCl...):40 wt% MgCl$_2$	7.82×10^{-6}

Fig. 5 Nyquist plot of (a) 70 wt% P(VdCl...): 30 wt% MgCl$_2$: 0.1 wt% SN, (b) 70 wt% P(VdCl...): 30 wt% MgCl$_2$: 0.2 wt% SN, (c) 70 wt% P(VdCl...): 30 wt% MgCl$_2$: 0.3 wt% SN and (d) 70 wt% P(VdCl...): 30 wt% MgCl$_2$: 0.4 wt% SN

Table 3 Conductivity values of plasticized polymer electrolytes calculated from Nyquist plot

Compositions	Ionic conductivity (σ) at room temperature S cm^{-1}
70 wt% P(VdCl...):30 wt% MgCl$_2$	1.89×10^{-5}
70 wt% P(VdCl...):30 wt% MgCl$_2$:0.1 wt% SN	8.02×10^{-5}
70 wt% P(VdCl...):30 wt% MgCl$_2$:0.2 wt% SN	1.55×10^{-4}
70 wt% P(VdCl...):30 wt% MgCl$_2$:0.3 wt% SN	1.42×10^{-3}
70 wt% P(VdCl...):30 wt% MgCl$_2$:0.4 wt% SN	9.19×10^{-4}

required for the systems to have the constant uniform ionic conductivity which is responsible for electrochemical devices operating over a wide range of temperature [48]. The regression values and the calculated values of activation energy are provided in Table 5. It can be seen that the activation energy decreases with increase
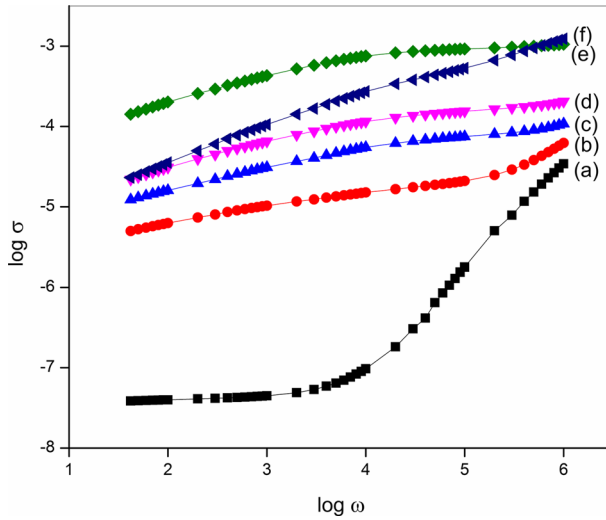
Fig. 6 Conductance spectra of (a) pure P(VdCl…), (b) 70 wt% P(VdCl…):30 wt% MgCl$_2$, (c) 70 wt% P(VdCl…): 30 wt% MgCl$_2$: 0.1 wt% SN, (d) 70 wt% P(VdCl…): 30 wt% MgCl$_2$: 0.2 wt% SN, (e) 70 wt% P(VdCl…): 30 wt% MgCl$_2$: 0.3 wt% SN, (f) 70 wt% P(VdCl…): 30 wt% MgCl$_2$: 0.4 wt% SN

Table 4 Comparison of conductivity values obtained from Nyquist plot and conductance spectra

Compositions	Ionic conductivity (σ) calculated from Nyquist plot S cm^{-1}	Ionic conductivity (σ) calculated from conductance spectra S cm^{-1}
Pure P(VdCl…)	3.07×10^{-8}	3.39×10^{-8}
70 wt% P(VdCl…):30 wt% MgCl$_2$	1.89×10^{-5}	1.62×10^{-5}
70 wt% P(VdCl…):30 wt% MgCl$_2$:0.1 wt% SN	8.02×10^{-5}	7.59×10^{-5}
70 wt% P(VdCl…):30 wt% MgCl$_2$:0.2 wt% SN	1.55×10^{-4}	1.58×10^{-4}
70 wt% P(VdCl…):30 wt% MgCl$_2$:0.3 wt% SN	1.42×10^{-3}	1.02×10^{-3}
70 wt% P(VdCl…):30 wt% MgCl$_2$:0.4 wt% SN	9.19×10^{-4}	8.69×10^{-4}

in the concentration of plasticizer in polymer electrolytes form 0.1 to 0.3 wt% SN, and then activation energy increases for 0.4 wt% SN. The increased amorphous nature provides a larger free volume in plasticized polymer electrolytes so that it has low activation energy. With the increase in amorphous nature, the polymer chain gets quicker internal modes in which bond rotation produces segmental motion to favor inter-chain hopping and intra-chain hoping so that the conductivity becomes high [49]. The lowest activation energy is observed for the electrolyte sample of
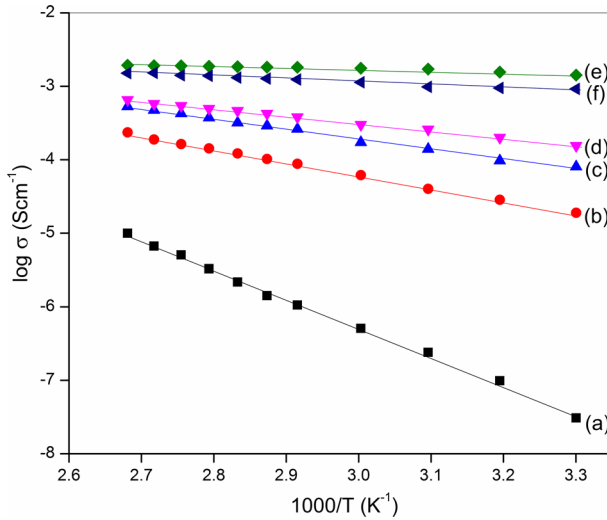
Fig. 7 Arrhenius plot of (a) pure P(VdCl…), (b) 70 wt% P(VdCl…):30 wt% MgCl$_2$, (c) 70 wt% P(VdCl…): 30 wt% MgCl$_2$: 0.1 wt% SN, (d) 70 wt% P(VdCl…): 30 wt% MgCl$_2$: 0.2 wt% SN, (e) 70 wt% P(VdCl…): 30 wt% MgCl$_2$: 0.3 wt% SN, (f) 70 wt% P(VdCl…): 30 wt% MgCl$_2$: 0.4 wt% SN

Table 5 Activation energy and regression value for prepared polymer electrolytes

Compositions	Activation energy in eV	Regression value
Pure P(VdCl…)	0.78	0.99
70 wt% P(VdCl…):30 wt% MgCl$_2$	0.62	0.98
70 wt% P(VdCl…):30 wt% MgCl$_2$:0.1 wt% SN	0.44	0.99
70 wt% P(VdCl…):30 wt% MgCl$_2$:0.2 wt% SN	0.28	0.97
70 wt% P(VdCl…):30 wt% MgCl$_2$:0.3 wt% SN	0.26	0.98
70 wt% P(VdCl…):30 wt% MgCl$_2$:0.4 wt% SN	0.32	0.97

highest conductivity having the polymer–salt–plasticizer composition as 70 wt% P(VdCl…):30 wt% MgCl$_2$:0.3 wt% SN.

Transference number measurements

Wagner's method

The contribution of charged species either ions or electrons involved during conduction in the electrolytes can be identified by transference number measurements. Wagner's DC polarization technique is employed to determine the total ion transport number for polymer electrolyte with stainless-steel electrodes. In this technique, the prepared plasticized polymer electrolyte of the highest conductivity has been
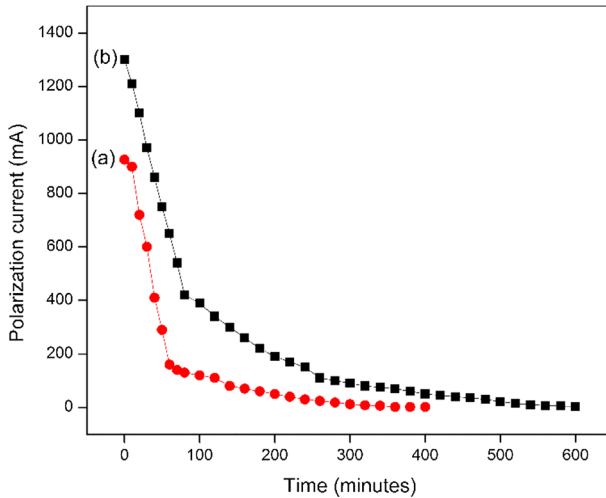
Fig. 8 Variation of polarization current in (a) SS │ SPE │ SS cell and (b) Mg │ SPE │ Mg cell

polarized with a fixed potential of 1.5 V using SS │ SPE │ SS cell arrangement, and the resulting polarization current flowing through the electrolyte due to the depletion of charged species is monitored as a function of time. Figure 8 shows the DC polarization current versus time plot of 70 wt% P(VdCl…):30 wt% MgCl$_2$:0.3 wt% SN-incorporated polymer electrolytes. It is evident that the plot exhibits high polarization current at the initial stage and then continue to fall off to reach a constant value after a long polarization period. The accumulation of mobile ions in the electrolyte surface nearer to the blocking electrodes (SS) occurs slowly, and after a certain time, the movement of ions is completely blocked by electrodes and the cell gets polarized [50]. The total ionic transference number (t_{ion}) of the polymer electrolytes is calculated by

$$t_{ion} = \frac{I_i - I_f}{I_i},$$

where I_i and I_f are the initial and final current, respectively. The t_{ion} value is determined as 0.99 confirms the major role of ions in the total conductivity of the polymer electrolyte.

Evan's method

The cationic transference number measurement is an important parameter to determine the performance of a polymer electrolyte with magnesium (Mg) electrodes. A combination of AC and DC technique on the Mg │ SPE │ Mg cell proposed by Evan's et al. [51] is implemented to determine the cationic transference number by measuring the bulk resistance of the Mg │ SPE │ Mg cell before and after polarization. The constant DC potential of 1.5 V is applied across the cell to polarize the polymer

electrolyte sample, accordingly the initial and final currents flowing through the cell are recorded at room temperature. AC impedance measurements have been made to determine the bulk resistance of the cell using the Nyquist plots before and after polarization. Cationic transference number (t_+) can be obtained from:

$$t_+ = \frac{I_s\left(V - I_0 R_0\right)}{I_0\left(V - I_s R_s\right)},$$

where I_0 is the initial current and I_s is the final current flowing through the sample on DC polarization. The variation of current as a function of time is shown in Fig. 8. R_0 is the bulk resistance before polarization and R_s is the bulk resistance of polarized cell obtained from Nyquist plot shown in Fig. 9 [41, 54]. The transference number that is calculated as 0.31 for the highest conducting sample 70 wt% P(VdCl…):30 wt% MgCl2:0.3 wt% SN shows that the significant contribution of Mg²⁺ ions in the total ionic conductivity of polymer electrolyte. Earlier, the transference number measurements by Evan's method for magnesium-based electrolytes are reported as 0.27 for poly(vinyl alchol)–poly(acrylonitrile) blend polymer electrolyte with magnesium per chlorate [52] and 0.31 for *I*-carrgeenan biopolymer electrolyte with magnesium nitrate [53].

Linear sweep voltammetry studies

Linear sweep voltammetry (LSV) experiment has been performed in order to study the electrochemical stability of the polymer electrolyte. The electrochemical stability of electrolyte is an important parameter which determines the operating voltage for electrochemical devices such as batteries [54]. The prepared plasticized polymer
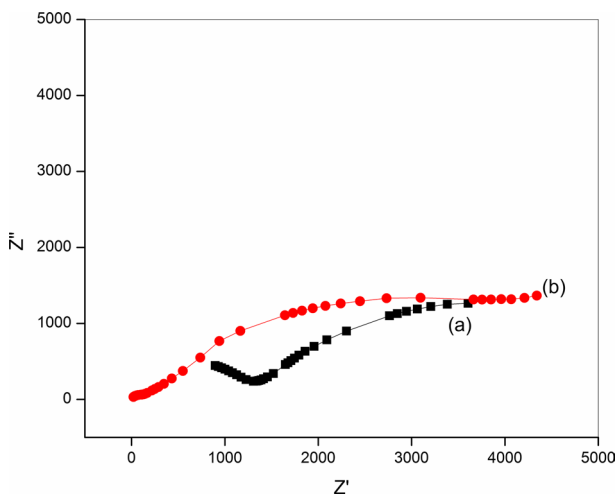

Fig. 9 Impedance plot of Mg │ SPE │ Mg cell (a) before polarization and (b) after polarization
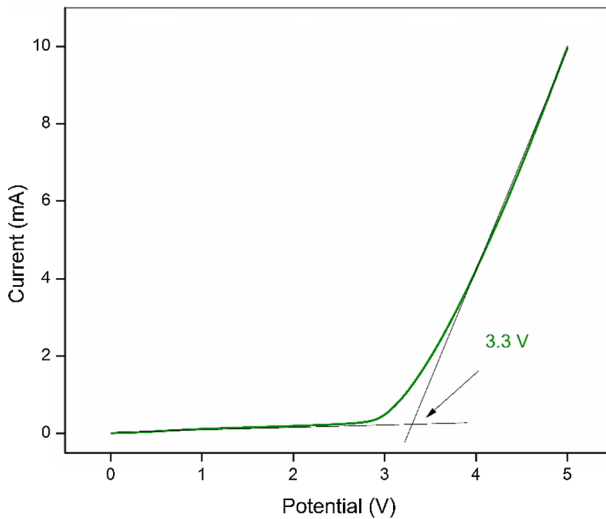
Fig. 10 Linear sweep voltammetry of highest conducting polymer electrolyte

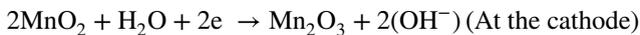electrolyte of highest conductivity is inserted between two stainless-steel (SS) electrodes so as to form a SS│SPE│SS cell arrangement and the current flow through the electrolyte for various voltages are measured at the scan rate of 1×10^{-3} V s^{-1}. From the characteristic curve shown in Fig. 10, it is observed that the initial potential is swept toward more anodic values until a rapid increase in current is obtained through the electrolyte. The high current is due to the decomposition at the inert electrode interface. The anodic decomposition voltage limit of the polymer electrolyte is defined as the potential at which a rapid rise in current is attained and continued to increase as the potential is swept and the initial current flow is associated with the decomposition of the given electrolyte [55, 56]. It is found that the current flow is stable up to 3.3 V which represents the electrochemical stability of electrolyte.

Battery performance test

A primary magnesium ion battery is constructed with magnesium metal plate as anode, manganese dioxide (MnO_2) doped with graphite as cathode, and prepared highest conductivity sample (70 wt% P(VdCl…):30 wt% $MgCl_2$:0.3 wt% SN) as electrolyte. The cathode material is prepared as a pallet by grinding MnO_2 with graphite in the ratio of 3:1 (MnO2: graphite) and pressed with 5-ton pressure. A primary battery is fabricated by sandwiching the prepared polymer electrolyte of the highest conductivity between anode and cathode materials. The parameters of the constructed cell are depicted in Table 6. A stable open-circuit voltage of 2.18 V across the anode and cathode is observed for a month, and Fig. 11 shows the voltage as a function of time.The anode and cathode reactions are given by:

Table 6 Cell parameters

Parameter	Measured values
Cell area (cm^2)	1.23
Effective cell diameter (cm)	1.2
Cell thickness (cm)	0.43
Cell weight (g)	1.34
Open-circuit voltage (V)	2.18
Current through 100 K (mA)	48
Power density (mW)	105
Discharge time through 100 K (h)	800
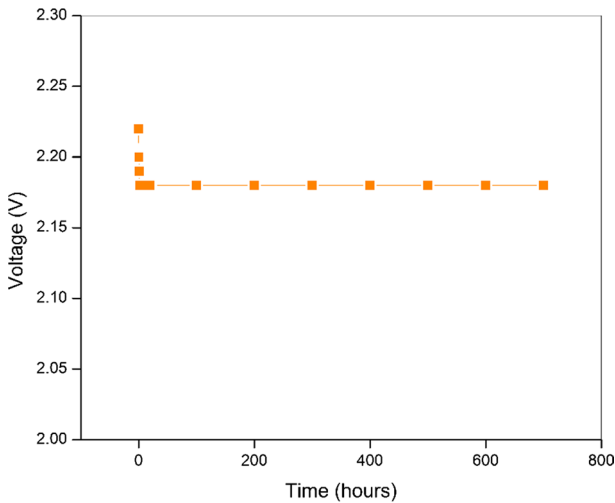
Fig. 11 Open-circuit voltage of primary battery (Mg │ SPE │ MnO$_2$ cathode)

$$Mg + 2(OH^-) \rightarrow Mg(OH)_2 + 2e \text{ (At the anode)}$$

$$2MnO_2 + H_2O + 2e \rightarrow Mn_2O_3 + 2(OH^-) \text{ (At the cathode)}$$

$$Mg + 2MnO_2 + H_2O \rightarrow Mg(OH)_2 + Mn_2O_3 \text{ (Overall reaction)}$$

In the above equations, existence of occluded moisture/H_2O in the polymer electrolyte membrane is the source of hydroxyl ions (OH^-). The non-essential water is present in the microscopic pores inside the polymer membrane due to the presence of physical forces [57].

The discharge characteristics of the battery are observed with the load of 100 KΩ. Initially, a steady voltage of 1.92 V is observed and the voltage reduced gradually to 1.84 V which remains stable for 10 days. Discharge performance of
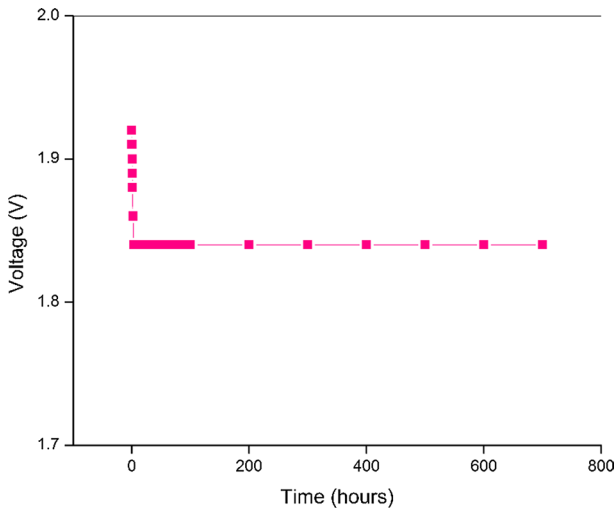
Fig. 12 Discharge characteristics of primary battery through 100 KΩ (Mg │ SPE │ MnO$_2$ cathode)

the battery is shown in Fig. 12. The initial decrease in voltage is ascribed to the self-discharge of primary magnesium battery [58]. Two constructed primary batteries are connected in series, and the output voltage is observed as 4.26 V. When light-emitting diode (LED) is connected across the batteries, the voltage dropped to 2.5 V and the current flow through LED is 204 mA. LED showed intense glow and the continuous glow is observed for 5 days as shown in Fig. 13.

Fig. 13 Series connection of constructed batteries makes LED glow

Conclusion

Most of the commercial batteries nowadays use lithium, but this may require low cost and safe materials for better environment to use the storage devices in electronic gadgets. This fundamental research involves in the development of magnesium batteries. poly(VdCl-*co*-AN-*co*-MMA) triblock copolymer, due to its considerable ionic conductivity, is identified as good electrolyte for magnesium ion batteries The polymer electrolytes using poly(VdCl-*co*-AN-*co*-MMA) with different concentrations of magnesium chloride have been prepared by solution-casting technique. The polymer electrolyte with the highest conductivity is identified and is found to be in the order of 10^{-5} S cm^{-1}. Addition of plasticizer succinonitrile with highest conducting polymer electrolyte sample increases the conductivity up to the order of 10^{-3} S cm^{-1}. XRD analysis shows the increase in amorphous nature of plasticized polymer due to the addition of magnesium salt and plasticizer. The decrease in glass transition temperature with increase in salt and plasticizer concentration is observed in DSC results. Higher amorphous nature and lower glass transition temperature imply increase in conductivity of polymer electrolyte. The transference number measurement shows the dominant contribution of cation (Mg^{2+}) in the overall conduction of the sample. The maximum stable open-circuit voltage of 2.18 V is attained with the constructed primary magnesium ion battery. The electrochemical stability of the electrolyte is determined as 3.3 V and is suitable choice for electrochemical devices.

References

1. Tan Y-H, Yao W-T, Zhang T, Ma T, Lei-Lei L, Zhou F, Yao H-B, Shu-Hong Yu (2018) High voltage magnesium-ion battery enabled by nanocluster Mg_3Bi_2 alloy anode in noncorrosive electrolyte. ACS Nano. https://doi.org/10.1021/acsnano.8b01847
2. Huie MM, Bock DC, Takeuchi ES, Marschilok AC, Takeuchi KJ (2015) Cathode materials for magnesium and magnesium-ion based batteries. Coord Chem Rev 287:15–27
3. Zhou L, Liu Q, Zhang Z, Zhang K, Xiong F, Tan S, An Q, Kang Y-M, Zhou Z, Mai L (2018) Interlayer-spacing-regulated VOPO$_4$ nanosheets with fast kinetics for high-capacity and durable rechargeable magnesium batteries. Adv Mater 30:1801984
4. Bančič T, Bitenc J, Pirnat K, Lautar AK, Grdadolnik J, Vitanova AR, Dominko R (2018) Electrochemical performance and redox mechanism of naphthalene-hydrazinediimide polymer as a cathode in magnesium battery. J Power Sour 395:25–30
5. Penki TR, Valurouthu G, Shivakumara S, Sethuraman VA, Munichandraiah N (2018) In-situ synthesis of bismuth (Bi)/reduced graphene oxide (RGO) nanocomposites as high capacity anode materials for Mg-ion battery. https://doi.org/10.1039/x0xx00000x
6. Saha P, Kanchan Datta M, Velikokhatnyi OI, Manivannan A, Alman D, Kumta PN (2014) Rechargeable magnesium battery: current status and key challenges for the future. https://doi.org/10.1016/j.pmatsci.2014.04.001
7. Zhao X, Zhao Z, Miao Y (2018) Chloride ion-doped polypyrrole nanocomposite as cathode material for rechargeable magnesium battery. https://doi.org/10.1016/j.materresbull.2018.01.012
8. Mesallam M, Sheha E, Kamar EM, Sharma N (2018) Graphene and magnesiated graphene as electrodes for magnesium ion batteries. https://doi.org/10.1016/j.matlet.2018.08.080
9. Nacimiento F, Cabello M, Pérez-Vicente C, Alcántara R, Lavela P, Ortiz GF, Tirado JL (2018) On the mechanism of magnesium storage in micro and nano-particulate tin battery electrodes. Nanomaterials 8:501

10. Zhang Z, Dong S, Cui Z, Du A, Li G, Cui G (2018) Rechargeable magnesium batteries using conversion-type cathodes: a perspective and minireview. Small Methods 1800020

11. Li Y, Yerian JA, Khan SA, Fedkiw PS (2006) Crosslinkable fumed silica-based nanocomposite electrolytes for rechargeable lithium batteries. J Power Sour 161:1288–1296

12. Hallinan DT Jr, Balsara NP (2013) Polymer electrolytes. Annu Rev Mater Res 43:503–525

13. Ahmad S (2009) Polymer electrolytes: characteristics and peculiarities. Ionics 15:309–321

14. Ibrahim S, Yassin MM, Ahmad R, Johan MR (2011) Effects of various LiPF$_6$ salt concentrations on PEO-based solid polymer electrolytes. Ionics 17:399–405

15. Meyer WH (1998) Polymer electrolytes for lithium-ion batteries. Adv Mater 10(6):439

16. Pandey M, Joshi GM, Ghosh NN (2016) Ionic conductivity and diffusion coefficient of barium-chloride-based polymer electrolyte with poly(vinyl alcohol)-poly(4-styrenesulphonic acid) polymer complex. Bull Mater Sci 40:655–666

17. Khutia M, Joshi GM, Deshmukh K, Pandey M (2015) Optimization of dielectric constant of polycarbonate/polystyrene modified blend by ceramic metal oxide. Polym-Plast Technol Eng 54:383–389

18. Fergus JW (2010) Ceramic and polymeric solid electrolytes for lithium-ion batteries. J Power Sour 195:4554–4569

19. Zhang Z, Fang S (2000) Novel network polymer electrolytes based on polysiloxane with internal plasticizer. Electrochim Acta 45:2131–2138

20. Soo PP, Huang B, Jang Y-I, Chiang Y-M, Sadoway DR, Mayes AM (1999) Rubbery block copolymer electrolytes for solid-state rechargeable lithium batteries. J Electrochem Soc 146(1):32–37

21. Arges CG, Kambe Y, Dolejsi M, Wu G, Segal-Pertz T, Ren J, Cao C, Craig GSW, Nealey PF (2017) Interconnected ionic domains enhance conductivity in microphase separated block copolymer electrolytes. https://doi.org/10.1039/c6ta10838e

22. Devaux D, Gle D, Phan TNT, Gigmes D, Giroud E, Deschamps M, Denoyel R, Bouchet R (2015) Optimization of block copolymer electrolytes for lithium metal batteries. https://doi.org/10.1021/acs.chemmater.5b01273

23. Saikia D, Hao-Yiang W, Pan Y-C, Lin C-P, Huang K-P, Chen K-N, Fey George TK, Kao H-M (2011) Highly conductive and electrochemically stable plasticized blend polymer electrolytes based on PVdF-HFP and triblock copolymer PPG-PEG-PPG diamine for Li-ion batteries. J Power Sourc 196:2826–2834

24. Young NP, Devaux D, Khurana R, Coates GW, Balsara NP (2014) Investigating polypropylene-poly(ethylene oxide)-polypropylene triblock copolymers as solid polymer electrolytes for lithium batteries. Solid State Ionics 263:87–94

25. Young W-S, Epps TH (2012) Ionic conductivities of block copolymer electrolytes with various conducting pathways: sample preparation and processing considerations. Macromolecules 45:4689–4697

26. Bouchet R, Phan TNT, Beaudoin E, Devaux D, Davidson P, Bertin D, Denoyel R (2014) Charge transport in nanostructured PS–PEO–PS triblock copolymer electrolytes. Macromolecules 47:2659–2665

27. Inceoglu S, Rojas AA, Didier Devaux X, Chen C, Stone GM, Balsara NP (2014) Morphology–conductivity relationship of single-ion-conducting block copolymer electrolytes for lithium batteries. ACS Macro Lett 3:510–514

28. Renaud Bouchet, Sébastien Maria, Rachid Meziane, Abdelmaula Aboulaich, Livie Lienafa, Jean-Pierre Bonnet, Trang N. T. Phan, Denis Bertin, Didier Gigmes, Didier Devaux, Renaud Denoyel, Michel Armand (2013) Single-ion BAB triblock copolymers as highly efficient electrolytes for lithium-metal batteries. https://doi.org/10.1038/nmat3602

29. Inbavalli D, Selvasekarapandian S, Sanjeeviraja C, Baskaran R, Kawamura J, Masuda Y (2013) Structural, thermal, morphological and electrical conductivity analysis of proton conducting tri block copolymer P(VdCl-Co-AN-Co-MMA) based electrolytes. In. J Electroact Mater 1:71–78

30. Inbavalli D, Selvasekarapandian S, Sanjeeviraja C et al (2015) Analysis of P(VdCl-co-AN-co-MMA)-LiClO4-EC triblock copolymer electrolytes. Bull Mater Sci 38:183

31. Inbavalli D, Selvasekarapandian S, Sanjeeviraja C et al (2013) Analysis of lithium ion conducting P(VdCl-co-AN-co-MMA)-LiClO4-DMF tri block copolymer electrolytes. Indian J Appl Res 3(12). ISSN-2249-555X

32. Anbazhakan K, Selvasekarapandiyan S, Monisha S et al (2017) Lithium ion conductivity and dielectric properties of P(VdCl-co-AN-co-MMA)-LiCl-EC triblock co-polymer electrolytes. Ionics 23:2663

33. Pandey M, Joshi GM, Ghosh NN (2016) Electrical performance of lithium ion based polymer electrolyte with polyethylene glycol and polyvinyl alcohol network. Int J Polym Mater Polym Biomater 65:759–768

34. Eom H-C, Park H, Yoon H-S (2010) Preparation of anhydrous magnesium chloride from ammonium magnesium chloride hexahydrate. Adv Powder Technol 21:125–130

35. Zhang Z, Xuchen L, Yang S, Pan F (2012) Preparation of anhydrous magnesium chloride from magnesia. Ind Eng Chem Res 51:9713–9718

36. Hodge RM (1996) Water absorption and states of water in semicrystalline poly(vinyl alcohol) films. Polymer 37(8):1371–1376

37. Rahman MYA, Ahmad A, Lee TK, Farina Y, Dahlan HM (2012) LiClO$_4$ salt concentration effect on the properties of PVC-modified low molecular weight LENR50-based solid polymer electrolyte. J Appl Polym Sci 124:2227–2233

38. Polu AR, Kumar R (2013) Ionic conductivity and discharge characteristic studies of PVA-Mg(CH$_3$COO)$_2$ solid polymer electrolytes. Int J Polym Mater Polym Biomater 62(2):76–80

39. Polu AR, Kumar R (2013) Preparation and characterization of PVA based solid polymer electrolytes for electrochemical cell applications. Chin J Polym Sci 31(4):641–648

40. Selvalakshmi S, Vijaya N, Selvasekarapandian S, Premalatha M (2016) Biopolymer agar-agar doped with NH$_4$SCN as solid polymer electrolyte for electrochemical cell application. J Appl Polym Sci. https://doi.org/10.1002/APP.44702

41. Liu W, Lee SW, Lin D, Shi F, Wang S, Sendek AD, Cui Y (2017) Enhancing ionic conductivity in composite polymer electrolytes with well-aligned ceramic nanowires. Nat Energy 2. Article number: 17035

42. Boukamp BA (1986) A package for Impedance/Admittance data analysis. Solid State Ion 18 & 19:136–140

43. Boukamp BA (1986) A Nonlinear least squares fit procedure for analysis of immittance data of electrochemical systems. Solid State Ion 20:31–44

44. Osman Z, Zainol NH, Samin SM, Chong WG, Md Isa KB, Othman L, Supa'at I, Sonsudin F (2014) Electrochemical impedance spectroscopy studies of magnesium-based polymethylmethacrylate gel polymer electroytes. ElectrochimicaActa 131:148–153

45. Kumudu Perera MAKL, Dissanayake PWSK Bandaranayake (2004) Ionic conductivity of a gel polymer electrolyte based on Mg(ClO$_4$)$_2$ and polyacrylonitrile (PAN). Mater Res Bull 39:1745–1751

46. Mathew CM, Kesavan K, Rajendran S (2014) Structural and electrochemical analysis of PMMA based gel electrolyte membranes. Int J Electrochem 2015. Article ID 494308

47. Aravindan V, Vickraman P (2007) A novel gel electrolyte with lithium difluoro(oxalato)borate salt and Sb$_2$O$_3$ nanoparticles for lithium ion batteries. Solid State Sci 9:1069–1073

48. Cowie JMG, Spence GH (1998) Ion conduction in macroporous polyethylene film doped with electrolytes. Solid State Ion 109:139–144

49. Tsunemi K, Ohno H, Tsuchida E (1983) A mechanism of ionic conduction of poly(vinylidene fluoride) lithium perchlorate hybrid films. Electrochimica 28(6):833–837

50. Muchakayala R, Song S, Gao S, Wang X, Fan Y (2017) Structure and ion transport in an ethylene carbonate-modified biodegradable gel polymer electrolyte. Polym Test 58:116–125

51. Evans J, Vincent CA, Bruce PG (1987) Electrochemical measurement of transference numbers in polymer electrolytes. Polymer 28:2324–2328

52. Manjuladevi R, Thamilselvan M, Selvasekarapandian S, Mangalam R, Premalatha M, Monisha S (2017) Mg-ion conducting blend polymer electrolyte based on poly(vinyl alcohol)-poly(acrylonitrile) with magnesium perchlorate. Solid State Ion 308:90–100

53. ShanmugaPriya S, Karthika M, Selvasekarapandian S, Manjuladevi R (2018) Preparation and characterization of polymer electrolyte based on biopolymer I-Carrageenan with magnesium nitrate. Solid State Ion 327:136–149

54. Mokhtar M, Majlan EH, Ahmad A, Tasirin SM, Daud WRW (2018) Effect of ZnO filler on PVA-alkaline solid polymer electrolyte for aluminum-air battery applications. J Electrochem Soc 165(11):A2483–A2492

55. Hallinan DT, Jr AR, McGill B (2016) An electrochemical approach to measuring oxidative stability of solid polymer electrolytes for lithium batteries. Chem Eng Sci 154:34–41

56. Zhang Y, Zhao Y, Gosselink D, Chen P (2014) Synthesis of poly(ethylene-oxide)/nanoclay solid polymer electrolyte for all solid-state lithium/sulfur battery. Ionics. https://doi.org/10.1007/s11581-014-1176-2

57. Manjuladevi R, Selvasekarapandian S, Thamilselvan M, Mangalam R, Monisha, Christopher Selvin P (2018) A study on blend polymer electrolyte based on poly(vinyl alcohol)-poly(acrylonitrile) with magnesium nitrate for magnesium battery. Ionics. https://doi.org/10.1007/s11581-018-2500-z

58. Chung S-H, Manthiram A (2017) Lithium–sulfur batteries with the lowest self-discharge and the longest shelf life. ACS Energy Lett 2:1056–1061

Publisher's Note Springer Nature remains neutral with regard to jurisdictional claims in published maps and institutional affiliations.

Affiliations

T. Ponraj[1,2,3] · A. Ramalingam[1] · S. Selvasekarapandian[3,4] · S. R. Srikumar[5] · R. Manjuladevi[6]

✉ S. Selvasekarapandian
   sekarapandian@rediffmail.com

1   Department of Physics, Government Arts College, Udumalpet, TamilNadu, India

2   Department of Physics, Nallamuthu Gounder Mahalingam College, Pollachi, TamilNadu, India

3   Materials Research Center, Coimbatore, TamilNadu, India

4   Bharathiar University, Coimbatore, TamilNadu, India

5   Kalasalingam Academy of Research and Education, Srivilliputhur, TamilNadu, India

6   PSG College of Arts and Science, Coimbatore, TamilNadu, India